ITEP - 119

INSTITUTE OF THEORETICAL
AND EXPERIMENTAL PHYSICS

A.M.Badalyan, M.I.Polikarpov,
Yu.A.Simonov

COUPLED CHANNELS
IN THE DIFFERENT MODELS

MOSCOW 1980

УДК 530.I45:538.3 М-I6

Abstract

This is the fourth of a series of preprints, where we discuss all types of poles in the coupled channel problems in all sheets including: classification, how the poles show up in the S-matrix and how they arise and how they more when the channel coupling is changing. Many numerical examples and several fits to the experimental data provided. The special case of resonance plus particle channels is considered exemplified by A_1 and Q-resonances. For the convenience of the reader we adopt a continuous numeration of sections, formulaes and references through all series of preprints.

А.М.Бадалян, М.И.Поликарпов, Ю.А.Симонов
Различные модели связанных каналов
Работа поступила в ОНТИ 5/УШ-I980г.

Подписано к печати II/УШ-80г. Т-I5222. Формат 70xI08 I/I6.
Печ.л.3,5.Тираж 290 экз.Заказ II9.Цена 26 коп.Индекс 3624.

Отдел научно-технической информации ИТЭФ,II7259,Москва

Notations and abbreviations

a_B	- the Bohr radius
BW (pole)	- the Breit-Wigner pole
BS	- bound state
CC	- the channel coupling
CC pole	- the coupled channel pole
E_i	- the threshold of the i-th channel in the the energy plane
μ (μ_i)	- reduced mass (in the channel i)
ERA	- effective range approximation
ERE	- effective range expansion
IVS	- inelastic virtual state
SSA	- the small shift approximation
UBS	- unstable bound state
UR	- the unitary relation
ZRA	- the zero range approximation.

The coupled channels in the different models

In this part for the description of the multichannel phenomena due to the channel coupling we consider the different methods: (1) the relativistic Logunov-Tavkhelidze--Blankenbecler-Sugar equations; (2) the Shrödinger equation with the separable potentials and (3) the many-channel N/D method. Below we make an emphasis on the dependence of pole trajectories and cross sections on the parameters of the CC interaction. In particular we consider in detail the properties of the $N\bar{N}$ system with the annihilation taken into account.

1. The coupled channels in the integral equation method

We follow in this Section the paper [36] where the relativistic two channel Logunov-Tavkhelidze-Blankenbecler--Sugar equations have been used. Two channel equations also in this case can be reduced in the exact way to the one channel equation with an effective interaction comprising the influence of another channel on a given one. The equation for the t-matrix has the form:

$$t_\ell(p,p',E)=V_\ell(p,p',E)+\frac{\pi}{2}\int_0^\infty \frac{dp''\, V_\ell(p,p'',E)\,t_\ell(p'',p',E)}{\sqrt{1+p''^2}\,(p''^2-E-i\varepsilon)} \qquad (4.1)$$

where two particles have the same mass M and units are such that $\hbar = M = C = 1$. The normalization of the t_ℓ is characterized by the on-shell value

$$t_\ell(p,p,p^2)=\frac{4}{\pi^2}\,p\sqrt{1+p^2}\;\frac{\eta e^{2i\delta}-1}{2i} \qquad (2)$$

The effective potential V_ℓ consists of two parts

$$V_\ell = V_{11} + V_{121} \qquad (3)$$

where V_{11} stands for the diagonal interaction in a given channel and V_{121} for the contribution of other channels (Fig. 1).

In a specific case of an interaction due to particle exchange, as shown in Figs. 1, 2, V_{11} and V_{121} can be written as

$$V_{11}=\lambda_1 Q_\ell\left(\frac{p^2+p'^2+m_1^2}{2pp'}\right)-\lambda_2 Q_\ell\left(\frac{p^2+p'^2+m_2^2}{2pp'}\right), \qquad (4)$$

$$V_{121}=\lambda\int_0^\infty \frac{\varkappa(\kappa)\,d\kappa}{(\kappa^2-E+E_t-i\varepsilon)}\,Q_\ell\left(\frac{p^2+\kappa^2+m_3^2}{2\kappa p}\right)Q_\ell\left(\frac{p'^2+\kappa^2+m_3^2}{2\kappa p'}\right) \qquad (5)$$

Here $\varkappa(k)$ is a phase space factor of intermediate particles of mass μ (see Fig. 1). We have neglected the interaction of these particles and consider them to be free. We also defined

$$p=\sqrt{E}=\sqrt{\tfrac{1}{4}s-1}\;;\quad E_t=\mu^2-M^2=\mu^2-1<0$$

The model was used to describe the $N\bar{N}$ interaction with annihilation taken into account (however the characteristic results below are quite general), in which case the phase space was taken as

$$\mathcal{R}(k) = \frac{1}{\sqrt{k^2+\mu^2}} \begin{cases} 1 + B(k^2+E_t) & \text{for } k^2+E_t > 0 \\ \left(-\frac{k^2}{E_t}\right)^{n_1} & \text{for } k^2+E_t \leq 0 \end{cases} \qquad (6)$$

The behaviour of $\mathcal{R}(k)$ was taken to imitate the multipionic phase space.

For two relativistic particles in channel 2 (two pions) $n_1 = B = 0$; in case of realistic annihilation which proceeds into 2-7 pions, n_1 was taken to be 2; two choices for B were considered; B=0 as for the two-body case and B=2, in which case $Im\, V_{121}(E=0) \cong Re\, V_{121}(E=0)$, i.e. $\gamma \cong 1$.

In actual calculations the angular momentum was l=0,1 and masses m_1, m_2 and m_3 were 770, 1500 and 939 MeV respectively. The parameters λ_1, λ_2 and λ have been varied to reproduce the elastic cross section $\sigma_{el}(E)$ and the annihilation cross section $v_{cm}\,\sigma_{inel}(E)$. The parameter μ was taken to be twice the pion mass.

Note, that the resulting values of λ_i can be compared with the OBEP values given by

$$\lambda_i = \frac{g_i^2}{2\pi^3} \quad , \; i = 1,2 \qquad (7)$$

and can qualitatively be understood in terms of the ω-exchanges for λ_1, ($g_\omega^2/4\pi \sim 10$) and the cut-off form factor for λ_2 ($\lambda_2 = \lambda_1$) .

The resulting trajectories for the poles of t-matrix in the sheet II are shown in Figs. 3 - 7 .

The trajectories in Fig. 3 correspond to a situation, when for $\lambda = 0$ there is a bound state, and B=2, so that

$\gamma = 1$, i.e. the CC interaction has an attractive real part. The trajectory of the UBB starts at the BB position (~ -200 MeV) and turns clockwise, passing the onset of the pionic cuts (the E_1 threshold) below threshold and going into upper half plane. In addition there is a CC pole which enters the second sheet from the sheet IV to the right from the threshold, makes a loop very closely to the threshold and the real axis (see the insertion above in Fig. .3.) and moves downwards with increasing λ .

To understand how the trajectory looks like when it start from a very deep BB, another case was investigated, shown in Fig. .4 . A BB poles is at -870 MeV, and the UBB trajectory tends steeply downwards. Again a CC pole emerges in Fig. 4 , which makes a loop and comes back closer to the real axis.

The trajectories of the CC poles for the case l=1 are shown in Figs. .5 and .6 . Note that larger values of λ_1 shift the trajectories to the left (more attracti - on).

For another set of parameters the trajectories are shown in Fig. .6 . Here the parameter B=2 while the curves in Fig. .5 correspond to B=0, therefore more attraction due to the channel coupling is present for the curves in Fig. .6 ; the latter are looping clockwise and the maximum width is smaller, than in the left curve in Fig. .5 Note that for small enough diagonal attraction and $\gamma < 1$ (corresponding to B=0) the CC pole tends to the right - see the right curve in Fig. .5

As was mentioned above, the CC trajectories enter the sheet II from the sheet IV, however the poles cannot be

found in the sheet IV in the present method without deformation of the integration path in (.1).

Therefore we do not know whether the poles we discuss originate from the distant singularities (in which case we can call them properly the CC poles) or from the BW* poles. In the case l=0 there are no BW and BW* poles for without channel coupling, therefore we are dealing with the CC-poles indeed; however for l=1 there is a BW pole and a BW* pole at $\sim 45 \pm 115$ MeV for $\lambda = 0$. It is very likely that all CC trajectories for l=1 shown in Fig. .5 and .6 originate from that BW* pole and therefore more properly should be called the BW* trajectories.

Very similar BW* trajectories are found for l=1 in the N/D method, they are discussed in Section 3. One remark characterizes the specific features of the model used in this Section.

The present model provides more than one CC pole with increasing λ . For $\lambda \geq 6$ and l=0 another CC pole appears (in addition to the shown in Fig. .4) which moves to the right with increasing λ reaching the position $E \cong 200 - i40$ MeV for $\lambda \cong 11$. Moreover, the behaviour of $v_{cm}\, \sigma_{an}(E)$ with E fixed and $\lambda \to \infty$ is the oscillation below and close to the unitary limit , which means that CC poles one after another emerge into the sheet II with increasing λ . This feature, probably is due to the local CC interaction, present in the model, while in the models with separable CC interaction one usually encounters one CC pole and a finite number of distant poles.

The accuracy of the effective range approximation which was shown to be so simple and powerful in the Parts 1,2 can be

easily checked in the model. The Fig. .7 shows $\alpha(E)$ and $\beta(E)$ for l=1 together with the inelasticity parameter $\eta(E)$ and the elastic and the inelastic cross sections. Here $\alpha(E)$ and $\tilde{\beta}(E)$ have been computed as functions of energy from the t-matrix t_ℓ (.2) using (1.39) with $\beta \rho_1 \to \tilde{\beta}$. Note that $\alpha(E)$ and $\tilde{\beta}(E)$ are very close to the straight lines, assuming that the effective range approximation is fairly good in this case. A similar result will be found in the N/D calculations in Section .3 On a whole, all the qualitative results of the present model are similar to the results of other models considered in parts 3,4 except for a remark given above.

.2 Separable and other models

From now on we denote the channel of heavy particles as channel 1.

The number of papers denoted to the derivation of the many channel equations and their solutions is very large. Therefore we consider only those papers which illustrate the properties discussed in the present review.

One of the first models used for dynamical calculations in many channels was the model of the square well potentials. When all radii of the wells both in diagonal and in the CC potentials are the same, the problem simplifies and the answer is given in a general form [8,17]. Extensive studies of the cross sections for several choices of the well depth are done by Fonda and Newton [16]. In the example of the $\Lambda p - \Sigma N$ coupled channels a cusp at the threshold appears for a specific choice of the square well parame -

ters [16], which probably signifies the presence of a pole near the ΣN threshold (see discussion in the Part 2). No trajectories are presented in the cited papers however.

Another class of solvable many channel problems contains separable potentials both for diagonal and nondiagonal (CC) interactions [105]. These models are used in nuclear physics [106] and in the particle physics, e.g. for the ΛN system [107]. The same type of models with the three-body channels has been applied for the interaction of Λ and Σ with nuclei [108], protons with nuclei [109] and also for the deutron stripping [110].

Several exactly solvable models are considered in [97], the same models have been applied to study different definitions of the concept of the resonance in [63].

Solution of the many channel equations also simplifies if the CC interaction alone is separable, while the diagonal interaction is arbitrary. These models are used in the study of the nucleon-nucleus scattering [111]. In nuclear physics for the CC interaction the δ-function potentials are exploited [112]; e.g. for the neutron scattering off ^{15}N [113] and ^{12}C [114].

At present there are some many channel calculations with local potentials for diagonal and CC interactions, e.g. Woods-Saxon type potentials have been used for the neutron scattering off ^{12}C [115], the OBE potentials have been exploited for the $\Lambda\bar{\Lambda} - \Sigma\bar{\Sigma}$ system [116] and for the $D\bar{D} - D^*\bar{D}^*$ system [117].

The theory of the many-channel reactions in nuclear physics has been treated in the review paper by Tamura [9], some aspects of this theory are discussed in [118] and [119].

We also mention a series of papers where different many channel equations have been derived [120]. In all the listed above papers, with exclusion of [119] the trajectories of the poles with varying CC interaction are not considered. For small CC interaction the trajectories are discussed in the framework of the two channel model in [121] and in the many-channel model in [122]. In both papers the separable potentials have been used.

In what follows we focus our attention on the papers where the pole trajectories have been studied.

Quantanilla and Mello considered the square well potential as diagonal interaction and the separable with the square well form factors for the CC interaction [123], in which case the S-matrix can be written in an analytic way. They have studied the BW trajectories as functions of the channel coupling and found that these may come very close to the real axis. For example one pole trajectory comes to the position $Ka = 4.95 - 0.09i$ and for some larger channel coupling another trajectory comes to the position $Ka = 8.55 - 0.09i$.

A rather extensive study of two and three channel problem with the separable potentials of the Yamaguchi type, was done by Karlsson and Kerbikov [99]. Their model is devised to describe the $N\bar{N}$ system with annihilation simulated by two heavy bosons; therefore the specific feature is that the radius of the CC potential is much smaller than the radius of the diagonal $N\bar{N}$ potential. The diagonal interaction is present only in the channel 1 ($N\bar{N}$) and is fixed by the prescribed value of the initial position of the bound state (when the CC interaction is switched off). In Fig. 7

and .8 we show the curves taken from [99], describing the trajectories of the UBS type starting from different positions E_o for CC coupling $\lambda = 0$. One can easily see that the trajectory of Fig. 7 belongs to the type of the UBS trajectories with $\gamma < \gamma_{cr}$, while the trajectory of Fig. .8 is characteristic for those with $\gamma > \gamma_{cr}$, considered in Section 3.4 and 3.5. To understand this difference let us write the equivalent optical potential in the channel 1 (we keep notations of ref. [99]):

$$V_{121} = -\lambda^2 |\beta\rangle \langle\beta| G_2(E) |\beta\rangle \langle\beta| \qquad (.8)$$

where $|\beta\rangle$ refers to the CC separable interaction:

$$\langle r|\beta\rangle = \sqrt{2\beta}\, r^{-1} \exp(-\beta r) \qquad (.9)$$

and

$$\langle\beta| G_2(E) |\beta\rangle = \frac{1}{(\beta - iK_2)^2} \qquad (.10)$$

Therefore the ratio of the real to the imaginary part of the optical potential (3.72) is

$$\gamma \equiv \frac{Re\, V_{121}}{Im\, V_{121}} = \frac{\beta^2 - K_2^2}{2\beta K_2} \qquad (.11)$$

with $K_2 = \{m_2 [2(m_1 - m_2) + E]\}^{1/2}$.

From (11) we see that γ depends on the energy E and for the trajectories beginning at some E_o around the threshold E_2 (when $K_2 = 0$), γ is large and positive, $\gamma > \gamma_{cr}$. This fact explains the form of the trajectory in Fig. 8. On the other hand, for the trajectories beginning near the first ($N\bar{N}$) threshold, E = 0, γ is small

and passes through zero at $\beta^2 = \kappa_2^2$. In this way we can understand the trajectory of Fig. 7 , where γ appears to be less than γ_{cr} . Similar considerations apply to the trajectories of the three-channel case, considered in [99].

Three body channel in the K-harmonics formalism [124] coupled by a separable potential to a two body channel was considered in [125] with the result that trajectories loop clockwise, i.e. they correspond to the case $\gamma > \gamma_{cr}$. This is a consequence of the 3 body phase space growing faster than the 2 body, which fact was already mentioned in [39].

The separable V_{11} and V_{12} with $V_{22} = 0$ have been used by Kudryavtsev and Tyapaev [126] to study the trajectories of the BW type. They show that the part of the trajectory with small enough λ near the threshold E=0 can be described by an equation:

$$E = E_R - \frac{i\Gamma}{2} + \lambda^2 A e^{i\varphi} \qquad (.12)$$

with $A > 0$ and

$$\varphi = \pi - \operatorname{arctg}\frac{\Gamma}{2E_R} + 2\operatorname{arctg}\frac{\sqrt{2m_2(m_1-m_2)}}{\beta} \qquad (13)$$

Therefore for wide enough BW resonances such that

$$\operatorname{arctg}\frac{\Gamma}{2E_R} > \delta \equiv 2\operatorname{arctg}\frac{\sqrt{2m_2(m_1-m_2)}}{\beta}, \qquad (.14)$$

the trajectory tends upwards and the CC interaction makes the resonance more narrow, whereas in the opposite case

$$\operatorname{arctg}\frac{\Gamma}{2E_R} < \delta \qquad (15)$$

the resonances due to the CC interaction become wider. Examples of both type of trajectories are given in [126]. We shall discuss this question in more detail in the part 5 of this review.

An extensive study of the two channel problem with V_{11} as a superposition of the Yukawa potentials and a separable interaction for V_{12}, while $V_{22} = 0$, has been done in [127]. The URS trajectories are shown to be sensitive to the amount of the short range repulsion, and a IVS trajectory was found close to the threshold for nonrepulsive at origin V_{11}, while it is very distant from the threshold for a repulsive at origin V_{11}.

In [128] the energy shifts of the levels in the system $\Sigma\bar{\Sigma}$ $(\Lambda\bar{\Lambda})$ due to the coupling to the $N\bar{N}$ channel have been considered. The annihilation to the pionic channels have been disregarded.

3. The coupled channels in the N/D method

A. General formalism:

The N/D method allows one to obtain a general solution of the unitary relation (1.7) with a prescribed dynamical mechanism, given in a form of l.h.s. discontinuities of the amplitude $\hat{f}$. Originally introduced by Chew and Mandelstam [129] it was given the many channel formulation by Bjorken [130].

The amplitude $\hat{f}$ is written as:

$$\hat{f} = \hat{N} \cdot \hat{D}^{-1} \qquad (3.16)$$

and the following matrix equations for $\hat{N}$ and $\hat{D}$ hold:

$$\frac{1}{2i}\Delta\hat{N}(E) = \hat{\xi}(E)\hat{D}(E) \qquad (17)$$

$$\frac{1}{2i}\Delta\hat{D}(E) = -\hat{K}(E)\hat{N}(E) \qquad (18)$$

where $\hat{K}(E)$ is the diagonal phase space matrix and $\hat{\xi}(E) = \hat{\xi}^{T}(E)$ assumed to be a given matrix, describing the dynamics - the matrix of the l.h.s. discontinuities of all driving diagrams, representing all particle exchanges in the t- and u-channels.

In what follows we do not make distinction between two and many body channels (the latter are important in the annihilation processes). When the forces between the pions are neglected (see below) the present formalism applies also to the multipionic channels in a rigorous way resulting in the modification of the final phase space expression. For more details see [39, 45].

From (17)-(18) we deduce a nonsingular matrix equation for $\hat{N}$ or $\hat{D}$ only, e.g.

$$\hat{D}(E) = \hat{1} + \frac{1}{\pi}\int_{L} dE'\,\hat{R}(E,E')\hat{\xi}(E')\hat{D}(E'), \qquad (19)$$

where the diagonal matrix $\hat{R}$ is defined as

$$\hat{R}(E,E') = \frac{E-E_0}{\pi}\int_{E_{th}}^{\infty} dE''\,\frac{\hat{K}(E'')}{(E''-E)(E''-E_0)(E''-E')} \qquad (20)$$

and E_{th} is a threshold for a chosen channel i in $\hat{K}$, whereas E_0 is a subtraction point, $\hat{D}(E_0) = \hat{1}$.

In the most part of this Section we consider for simpli-

city the case, when the matrix $\hat{\xi}$ has the form:

$$\hat{\xi} = \begin{pmatrix} \xi_{11} & \xi_{12} & \dots & \xi_{1n} \\ \xi_{21} & 0 & \dots & 0 \\ \dots & \dots & \dots & \dots \\ \xi_{n1} & 0 & \dots & 0 \end{pmatrix} \qquad (21)$$

i.e. interaction is present only in the channel 1 and there is a CC interaction coupling channel 1 to all other channels. Then the n x n system (19) reduces to n equations for the elements D_{11} and D_{1j} (j = 2, ..., n) (see [39,45, 6]):

$$D_{11}(E) = 1 + \frac{1}{\pi}\int_L dE' K(E,E') D_{11}(E'), \qquad (22)$$

$$D_{1j}(E) = K_j^0(E) + \frac{1}{\pi}\int_L dE' K(E,E') D_{1j}(E') \qquad (23)$$

where

$$K(E,E') = K_{11}(E,E')\xi_{11}(E') + \frac{1}{\pi}\sum_{j=2}^{n}\xi_{j1}(E')\int_L dE'' R_{11}(E,E'') \times R_{1j}^0(E'',E')\xi_{1j}(E'') \qquad (24)$$

and

$$K_j^0(E) = \frac{1}{\pi}\int_L dE' R_{11}(E,E')\xi_{1j}(E') \qquad (25)$$

All other elements D_{kj} (k, j = 2, ..., n) and D_{j1} are expressed due to (19) through D_{11} and D_{1j}.

The matrix $\hat{N}$ is computed through $\hat{D}$ using the relation:

$$\hat{N}(E) = \frac{1}{\pi} \int_{4}^{\infty} \frac{dE'}{E'-E} \hat{S}(E') \hat{D}(E') \qquad (.26)$$

B. Application to the $N\bar{N}$ case.

We now return to the general case, given by eqs. (.22)-(.25). The channel 1 refers to $N\bar{N}$ and the energy is equal to $E = \frac{s - 4m_N^2}{4m_N}$.

The specific features of the $N\bar{N}$ channel are:

1) the annihilation takes place mainly through 3-7 pions;

2) the threshold of annihilation channels starts at $E \approx -m_N$, i.e. very far from the $N\bar{N}$ threshold;

3) the range of OBE forces in the $N\bar{N}$ channel is on average of the order of m_σ^{-1} and the corresponding l.h.s. cut of the amplitude starts at $E_x = -\frac{m_i^2}{4m_N}$, where m_i stands for the mass of the exchanged particle.

4) The range of annihilation can be calculated from the diagrams of Fig. .9 and is equal to $(2m_N)^{-1}$ [131]. The corresponding l.h.s. cuts in the amplitudes connecting $N\bar{N}$ to specific pionic channels start therefore far from the $N\bar{N}$ threshold: at $E_{an} \sim -m_N$ [36,39].

5) The interaction inside pionic channels can be considered as relative weak as compared with the CC interaction coupling pions to $N\bar{N}$. This fact can be checked by the inspection of the $\pi\pi$ amplitude [58]. The only effect of the pionic channels which may be of importance - existence of the S-channel resonances like ρ, ω - weakly affects our results near the $N\bar{N}$ threshold [45].

The singularity structure of the $N\bar{N}$ amplitudes is shown in Fig. 10. One notices the short gap between the "annihilation cut" (l.h.s. dynamic cut of the $N\bar{N} \to \pi\pi$, ... amplitudes) and the onset of the unitary cuts $E_{2\pi}$. It is there that the subtraction point E_0 is usually chosen to be.

We now do the following simplifications:

i) using the property 5) we neglect all interpionic l.h.s. cuts; in this way the matrix $\hat{\xi}$ assumes the form (21); ii) we replace all annihilation cuts by the pole terms, namely

$$\xi_{ij}(E) = \xi_{j1}(E) = \eta_i \delta(E - E_a) \quad (j = 2, \dots, n) \qquad (27)$$

This procedure may be justified by the fact that all annihilation cuts are far off the energy region of interest - the $N\bar{N}$ threshold - and therefore the detailed behaviour of ξ_{1j} is not impotrant. This last simplification is of technical character and can be easily improved if one has information on specific mesonic channels, which is absent at present.

We may now choose the subtraction point E_0 in the dispersion integrals for $\hat{D}(E)$, eqs. (19)-(20), to coincide with E_a : $E_0 = E_a$. In this way, again as in the previous Section, a great simplification occurs and everything can be expressed in terms of only two functions, $D_{11}(E)$ and $d(E)$:

$$D_{1j}(E) = \eta_j d(E); \quad D_{j1}(E) = \frac{1}{\pi} \eta_j R_{jj}(E, E_0), \qquad (28)$$
$$D_{kj}(E) = \delta_{kj} \quad (k, j = 2, \dots, n),$$

which satisfy the equations:

$$D_{11}(E) = 1 + \frac{1}{\pi}\int_{L} dE' R_{11}(E,E')\xi_{11}(E')D_{11}(E'), \qquad (29)$$

$$d(E) = \frac{1}{\pi}R_{11}(E,E_0) + \frac{1}{\pi}\int_{L} dE' R_{11}(E,E')\xi_{11}(E')d(E'). \qquad (30)$$

At the same time all η_j and R_{jj} combine into the effective pionic phase space integral $z(E)$ and effective CC coupling λ :

$$\lambda z(E) \equiv -\frac{1}{\pi}\sum_{j=2}^{n}\eta_j^2 R_{jj}(E,E_0) = \lambda\frac{E_0-E}{\pi^2}\int_{E_{th}}^{\infty} dE' \frac{\chi(E')}{(E'-E)(E'-E_0)^2} \qquad (31)$$

with the condition on the effective pionic phase space $\chi(E)$:

$$\chi(0) = 1.$$

In terms of these functions the determinant is

$$Det\,\hat{D}(E) = D_{11}(E) + d(E)\lambda z(E) \qquad (32)$$

and all observables can be expressed through the effective reaction matrix C [33-36,39] :

$$C = \tilde{N}\tilde{D}^{-1},$$

$$\tilde{D}(E) = \begin{bmatrix} D_{11} & d(E) \\ -\lambda z(E) & 1 \end{bmatrix}, \qquad (33)$$

$$\tilde{N}(E) = \begin{bmatrix} N_{11} & n(E) \\ \frac{1}{\pi(E_0-E)} & 0 \end{bmatrix}, \qquad (34)$$

where

$$N_{11}(E) = \frac{1}{\pi} \int_L \frac{dE'}{E'-E} \mathcal{F}_{11}(E') D_{11}(E') \qquad (.35)$$

and

$$n(E) = \frac{1}{\pi(E_0-E)} + \frac{1}{\pi} \int_L \frac{dE'}{E'-E} \mathcal{F}_{11}(E') dE' . \qquad (36)$$

With those definitions the averaged cross sections are:

$$\sigma_{an} = \frac{4\pi}{K} |C_{21}(E)|^2 \cdot \lambda \, x(E), \qquad (.37)$$

$$\sigma_{el} = 4\pi |C_{11}(E)|^2 . \qquad (.38)$$

In the definitions (.31) we have introduced a new parameter λ instead of many channel couplings η_{ℓ}. Another parameters is contained in the effective pionic phase space integral $z(E)$. Actually it is an unknown function of E, containing in principle infinitely many parameters, however we need it only nerr the $N\bar{N}$ threshold, where the imaginary part of $z(E)$ is fixed by the condition $x(0) = 1$ and only ratio of the real to the imaginary part of $z(E)$ is a new parameter. From the diagrammatic analysis one concludes that $z(E)$ is connected to the effective optical potential, replacing all the annihilation channels; we call it the annihilation potential V_{an}:

$$V_{an}(E) \equiv \sum_n V_{1n1}(E) = -\frac{4\lambda z(E)}{m_N (E_0 - E)} . \qquad (.39)$$

The properties of this potential may be deduced from the annihilation box diagram with n mesons in the inter-

mediate state, Fig. 9.

From that we deduce that i) $V_{an}(E)$ has ratio γ of the real to the imaginary axis of the order of unity;
ii) both γ and $Re\,V_{an}(E)$, $Im\,V_{an}(E)$ are slow functions of energy near the $N\bar{N}$ threshold;
iii) the value of $\lambda \sim 10^6$ in units of [33,36] corresponds to $g^2_{\pi NN}/4\pi$ = 14.5 in Fig. 9 with n=2,3,4,5.

All these properties are presented if we choose the effective pionic phase space in the form:

$$\chi(E) = \begin{cases} \left(\frac{E_{th} - E}{E_{th}}\right)^n, & E_{th} < E < 0 \\ 1 + AE, & E > 0, \end{cases} \qquad (40)$$

where n was taken equal 3 reproducing the threshold behaviour of 3 to 4 pions. For E_{th} we take the 4-pion threshold. The parameter A can be varied, the value

$$A = A_0 = -\frac{3}{E_{th}} \qquad (41)$$

corresponds to the smooth first derivative matching of $\chi(E)$ for E=0. It is interesting to note that γ is directly connected to A :

$$\gamma \equiv \frac{Re\,V_{an}}{Im\,V_{an}} = A\frac{|E_0|}{\pi} \qquad (42)$$

and therefore for $A = A_0$, $\gamma \cong 1$.

The behaviour of $Re\,V_{an}(E)$ and $Im\,V_{an}(E)$ when energy is around the $N\bar{N}$ threshold is shown in Fig. 11 for different values of A.

In this way we obtain two parameters λ and γ

with all other parameters (like E_{th}, E_o) fixed. It is imporrant to know that whatever the exact shape of $\chi(E)$ is only these two parameters essentially enter the problem. The sensitivity to the change of the fixed parameters was checked independently in [36,39].

The results are given in the following form: 1) the trajectories have been computed for the poles, corresponding to the zeros of the family of trajectories, on each trajecroty λ changes from 0 to infinity. 2) At the same time the cross sections $\sigma_{el}(p\bar{p})$, σ_{an} and $\sigma_{ex}(p\bar{p}\to n\bar{n})$ have been computed and fitted to the experimental data for different λ and γ. In this way the best fitted values λ and γ have been defined using only total cross sections, the best fit was obtained for $A = 3.24$ ($\gamma = 1$) and $\lambda = 0{,}7 \cdot 10^6$. Somewhat worse fit was obtained for $A = 6$ ($\gamma = 1.85$) and $\lambda = 0{,}45 \cdot 10^6$. Other checked values of λ and γ in the interval $-1 \leq \gamma < 4$, $0 \leq \lambda < \infty$ did not reproduce the cross sections.

3) The angular distributions can now be compared with experiment and give an additional check of consistency of that approach since no fitting parameters are involved there.

4) Finally for the fitted values of $\lambda = 0{,}7 \cdot 10^6$ and $\gamma = 1$ we define the position of all poles which are consistent with the experimentally observed cross sections.

Below we discuss the results in the given order 1)-4).

1. The trajectories. Sixteen amplitudes with $L \leq 2$, singlet, coupled and decoupled triplet waves have been searched for poles on all Riemann sheets connected to the $N\bar{N}$ threshold and the pionic threshold at E_{th}.

Since we have an effective two channel problem, classification of sheets and poles in what follows is relevant to the two channel notations. All essential pionic thresholds with number of pions up to eight lie far off to the left and therefore the pionic cut of the effective two channel problem plays the role of all pionic cuts of the original many channel problem.

Three types trajectories have been found.

The UBS-trajectories start from the BS or resonances of the isolated $N\bar{N}$ channel for $\lambda = 0$, as shown in Fig. 12 for the $^{11}S_0$ state, in Fig. 13 for $^{13}P_1$ state and in Fig. 14 for $^{11}D_2$ state. The curves in Fig. 12 correspond to $\gamma = 1.85;\ 1.23;\ 0.62;\ 0$ (A = 6, 4, 2 and 0) and are typical for the case $\gamma > \gamma_{cr}$. The P-wave trajectories in Fig. 13 for A = 6, 4; 2, 0, -2 are also of that type, while the left one for A = -4 ($\gamma = -1.23$) is typical for $\gamma < \gamma_{cr}$.

The P-wave trajectories in Fig. 14 are typical for wide initial resonances as we discussed in Section 2. Indeed the D-resonances seem to be so wide that attractive part of V_{an} deepens them and therefore made them more narrow.

Our resonances for l=2 seem to have wider elastic widths than those calculated by Dover et al. [132] for Paris potential. We must stress that elastic widths are very much model dependent since they can be expressed as the exponents of integrals over the barrier width and therefore are very sensitive to potential parameters.

The CC trajectories come nearby the $N\bar{N}$ threshold only for L=0, while for L≥1 they lie at a distance of more

than 200 MeV for all values of λ . The typical CC trajectories for $^{11}S_0$ state are shown in Fig. 15 for A = 8, 6, 4, 2 and 0 from top to bottom. The final point of all trajectories is at E = -12 MeV and corresponds to a zero of $d(E)$ (see eq. (.30)). For A < 0 the CC trajectory never comes close to the $N\bar{N}$ threshold, which means that $A \to 0$ ($\gamma \to 0$) is near the critical value of A (γ). The appearance of a CC pole near threshold is important in fitting the cross sections to large observed experimental values.

The CC trajectories come from the sheet IV and with growing λ enter the sheet II where they are shown in Fig. 15.

The BW and BW* trajectories. Both types occur in the states with L > 0, they start from a BW or a BW* resonance respectively. Note that a BW resonance lies (in our 2 channel equivalent case) in the sheet III while a BW* resonance lies in the sheet IV. Because of the specific topology of our two-channel Riemann surface the trajectories behave in a different way when the CC interaction is switched on. Namely, the BW* trajectory with increasing λ goes down, enters the sheet II to the right of the $N\bar{N}$ threshold and continues to go down in the sheet II. An example of that trajectory is shown in Fig. 16 for the $^{33}P_1$ state.

At the same time the BW trajectory stays on the sheet III and is going to the left with increasing λ for $\gamma > 0$, since increasing of λ in this case means effectively increasing of attraction. An example of a BW trajectory is shown in Fig. 17 for the $^{1}P_1$ (I=0) state.

Note that the BW* trajectories look like the CC trajectories in their location in the sheets and play the same

important rôle in fitting the cross sections.

2. The total cross sections are shown in Fig. 18 - 4.20 for elastic, charge exchange and annihilation cross sections respectively in the range 0 - 100 MeV. The fitting process is nontrivial since for three curves we have only two parameters λ and γ (or A) for all 16 partial waves. Nevertheless the quality of the fit is quite reasonable. Note the peaks in all cross sections at the threshold which result from the presence of the CC poles in the L=0 waves. No other peaks are seen in total or partial wave cross sections.

3. The angular distributions use already fitted in the total cross sections values $\lambda = 0{,}7 \cdot 10^6$ and $\gamma = 1$ $(A = 3{,}24)$ (in units of ref. [33-36]) and therefore do not contain any free parameters. The elastic cross section for E = 10 MeV is shown in Fig. 21 and for E = 50 MeV in Fig. 22, while the charge exchange cross section is shown in Fig. 23 for E = 100 MeV. The quality of the fit is in general good, some disagreement for $\cos\theta = -1$ and E = 50 MeV in Fig. 22 is probably due to the neglect of the waves with $L \geqslant 3$ which are specifically important in the backward region.

4. The position of the poles which is in agreement with the observed cross sections can now be listed from the calculated trajectories for fixed values of $\lambda = 0.7 \cdot 10^6$ and A = 3.24. The Table 1 shows 16 poles in different states for the case of no CC interaction ($\lambda = 0$) and the standard CC interaction ($\lambda = 0.7 \cdot 10^6$).

One can see that all resonances with $E_0 > 0$ have $\frac{\Gamma}{E_0} > 1$ which means that they hardly can be seen in the cross sec -

tions, as indeed the partial cross sections confirm.

For $E_o < 0$ three resonances appear in the S-waves near $E_o \cong -200$ MeV with $\frac{\Gamma}{E_o} \sim \frac{1}{2}$. They produce a broad bump in the hadronic ratio R [134].

Table 1 Pole positions with respect to the $N\bar{N}$ threshold (in MeV) obtained in the N/D method [35].

Isospin = 0			Isospin = 1		
State	λ =0	λ =0.7·10^{-6}	State	λ =0	λ =0.7·10^{-6}
$^1S_0$	-104	-199-57i	$^1S_0$	-115	-234-58i
$^3S_1$-$^3D_1$	- 95	-127-50i	$^3S_1$-$^3D_1$	- 86	-223-70i
$^3P_1$	- 26	-108-61i	$^3P_1$	7.7-46i	-6.4-12i
$^3P_0$	- 19	-40-37i	$^3P_0$	38-17i	-36-68i
$^1P_1$	5.5-2.8i	-5.4-8.6i	$^1P_1$	13-7i	-12-23i
$^3S_1$-$^3D_1$	68-177i	83-128i	$^3S_1$-$^3D_1$	62-79i	86-140i
$^1D_2$	74-107i	47-71i	$^1D_2$	108-122i	48-80i
$^3D_2$	146-59i	35-90i	$^3D_2$	75-120i	45-75i
$^1S_0$	-	8.8-0.2i	$^1S_0$	-	13.5-016i
$^3S_1$-$^3D_1$	-	*)	$^3S_1$-$^3D_1$	-	8.1-0.05i

*) No close by CC-pole found.

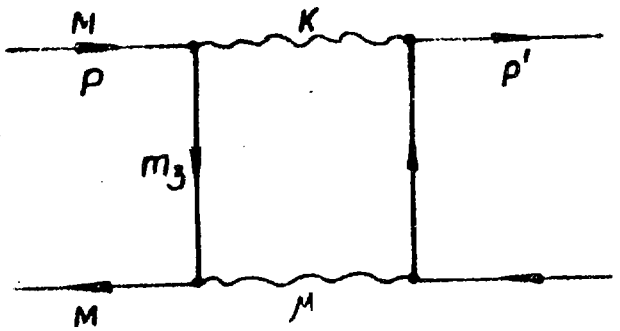

Fig.I. The annihilation box diagram, contributing to the effective potential V_3 .

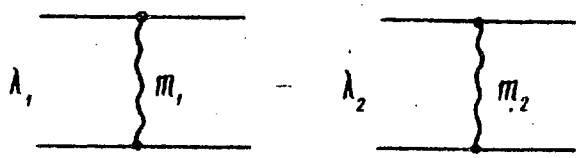

Fig.2. Graphical representation of the diogonal potential, entering the integral equation (I).

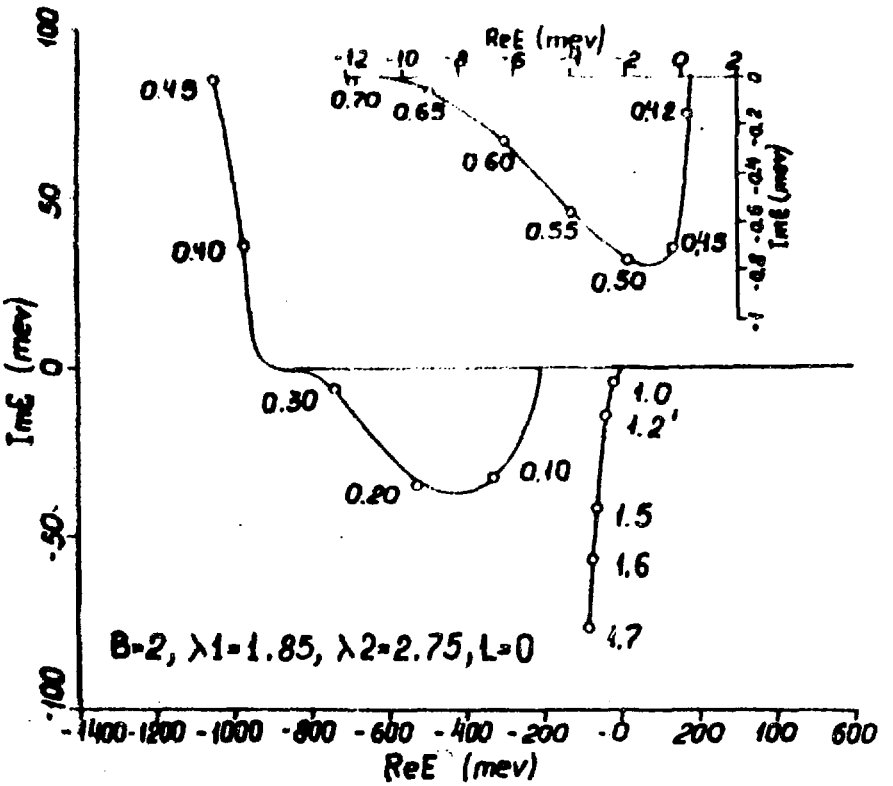

Fig. 3 The UBS (left) and the CC pole trajectories in the complex energy plane as a function of λ . Numbers at the curve are the values of λ .

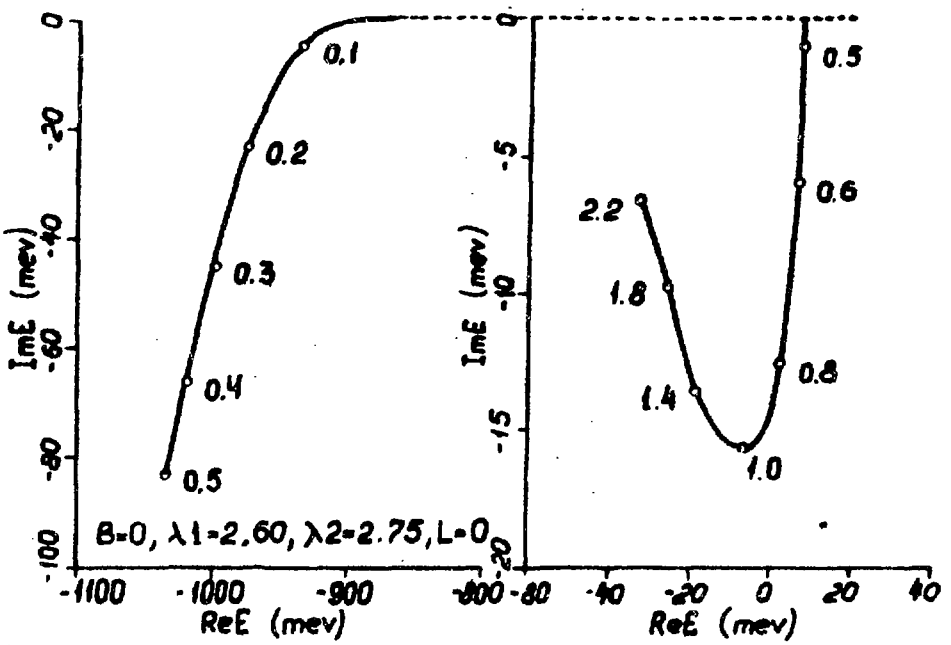

Fig. 4 As in Fig. 3 with the shown set of parameters.

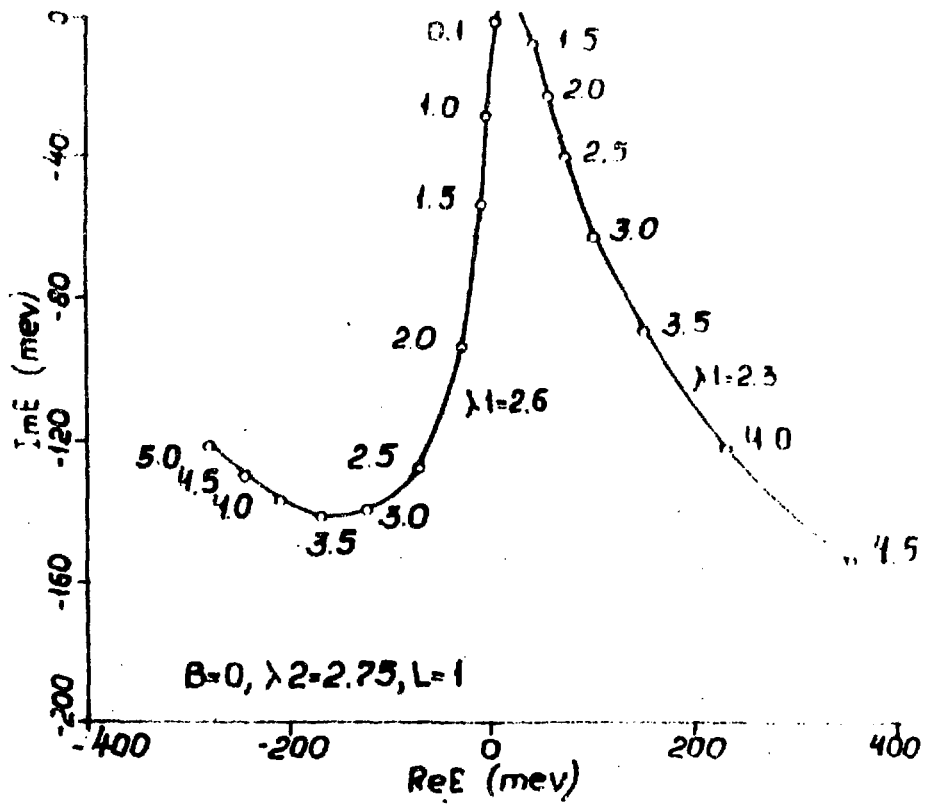

Fig. 5 . The trajectories of the CC poles for various sets of parameters.

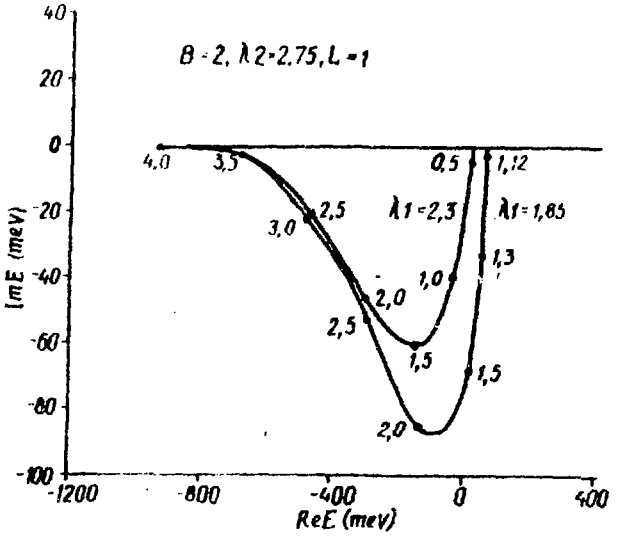

Fig. 6 As in Fig. 5 with the shown set of parameters.

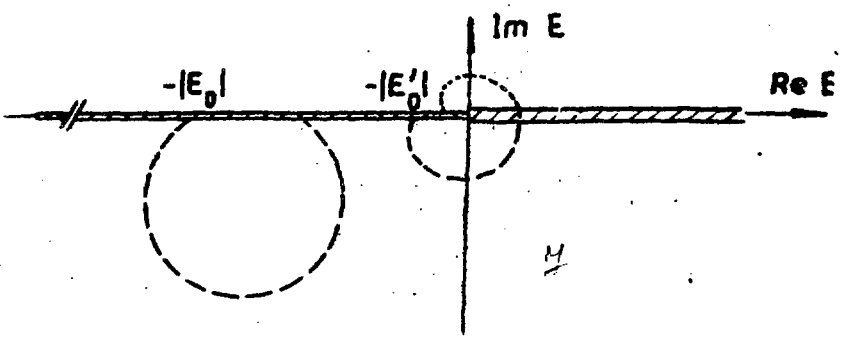

Fig. 7 The UBS trajectories with varying CC- interaction in the two-channel model with separable potentials [99].

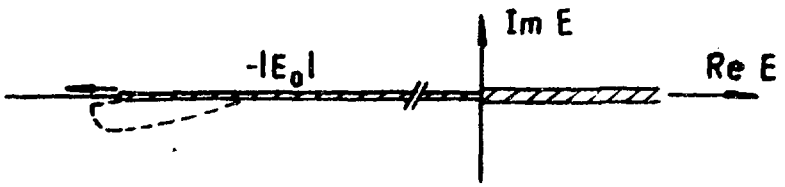

Fig. 8 | As in Fig. 7 for deeper initial BS.

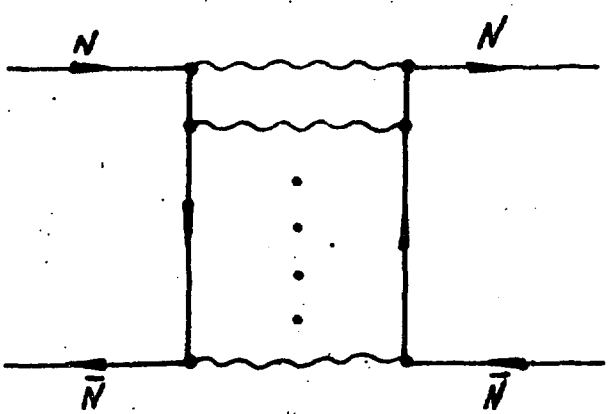

Fig. 9 | The box diagram, describing the $N\bar{N}$ annihilation into mesons (wavy lines).

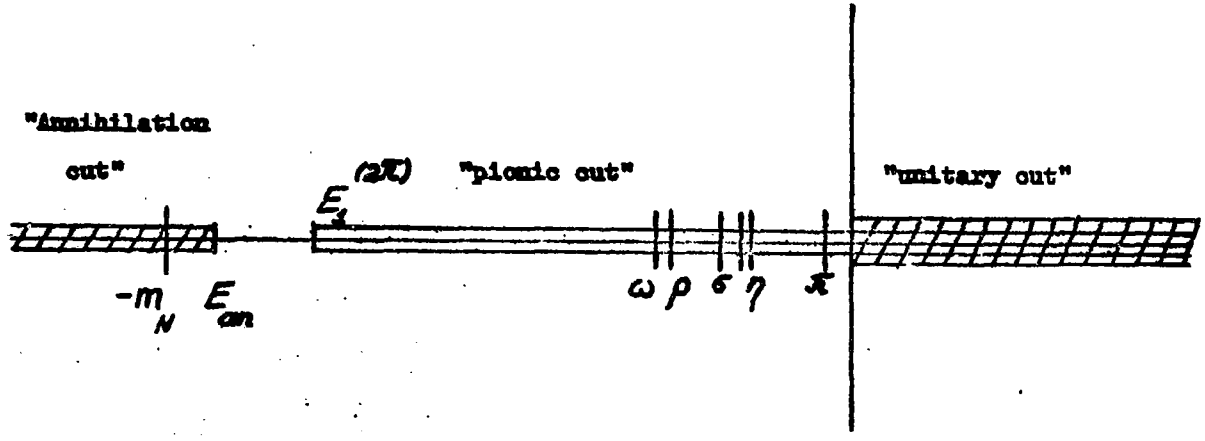

Fig. 10 Singularities of the $N\bar{N}$ amplitude in the energy plane. For the l.h.s. OBE cuts only the thresholds are shown.

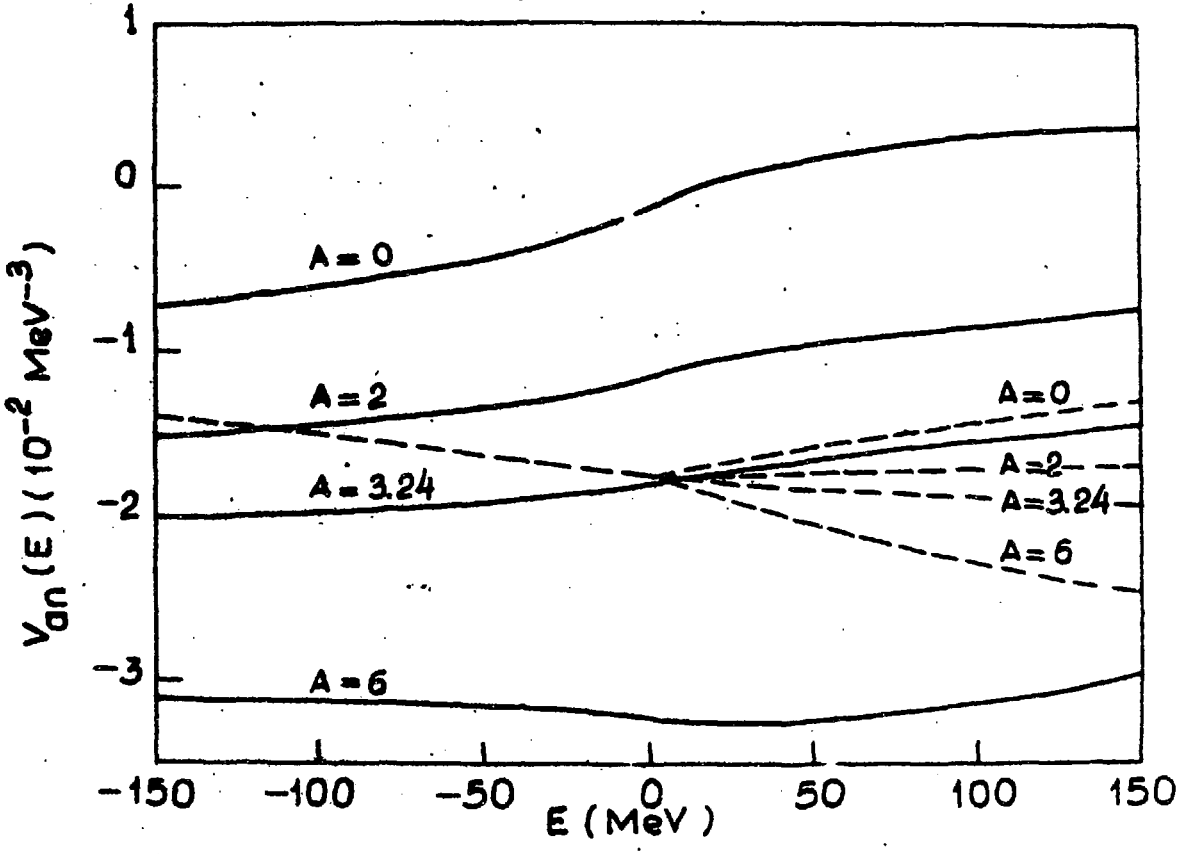

Fig. 11 The annihilation potential $V_{an}(E)$ for different values of A. Solid lines represent $Re\,V_{an}$, dashed lines $Im\,V_{an}$.

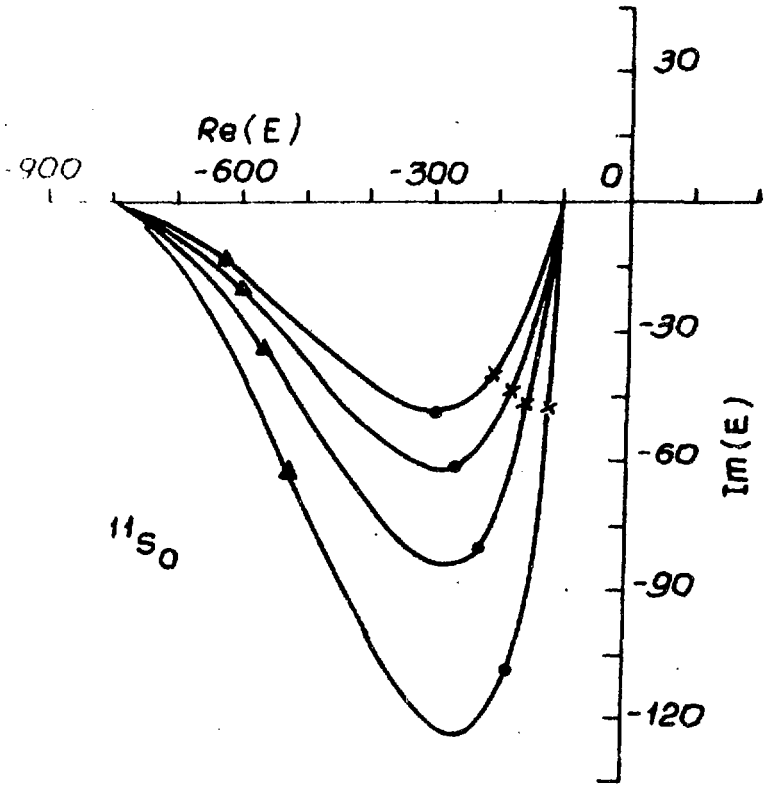

Fig. 12 The UBS trajectories from the N/D calculations in [35] for the $^{11}S_0$ - state in the energy plane (in MeV). Curves from top to bottom correspond to A = 6, 4, 2 and 0 respectively Positions corresponding to $\lambda = 0{,}5\cdot 10^6$; $1\cdot 10^6$ and 10×10^6 are marked by X , • and Δ respectively.

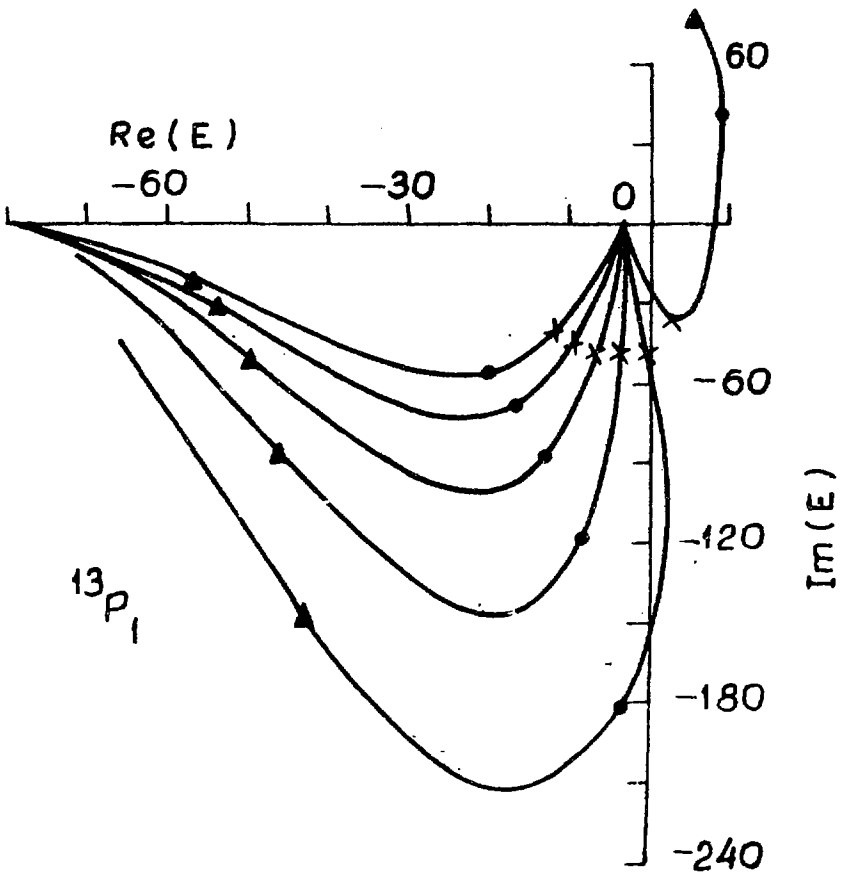

Fig. 13. As in Fig. 12 for $^{13}P_1$ - state. Curves from top to bottom correspond to A = 6, 4, 2, 0, -2 and -4 respectively.

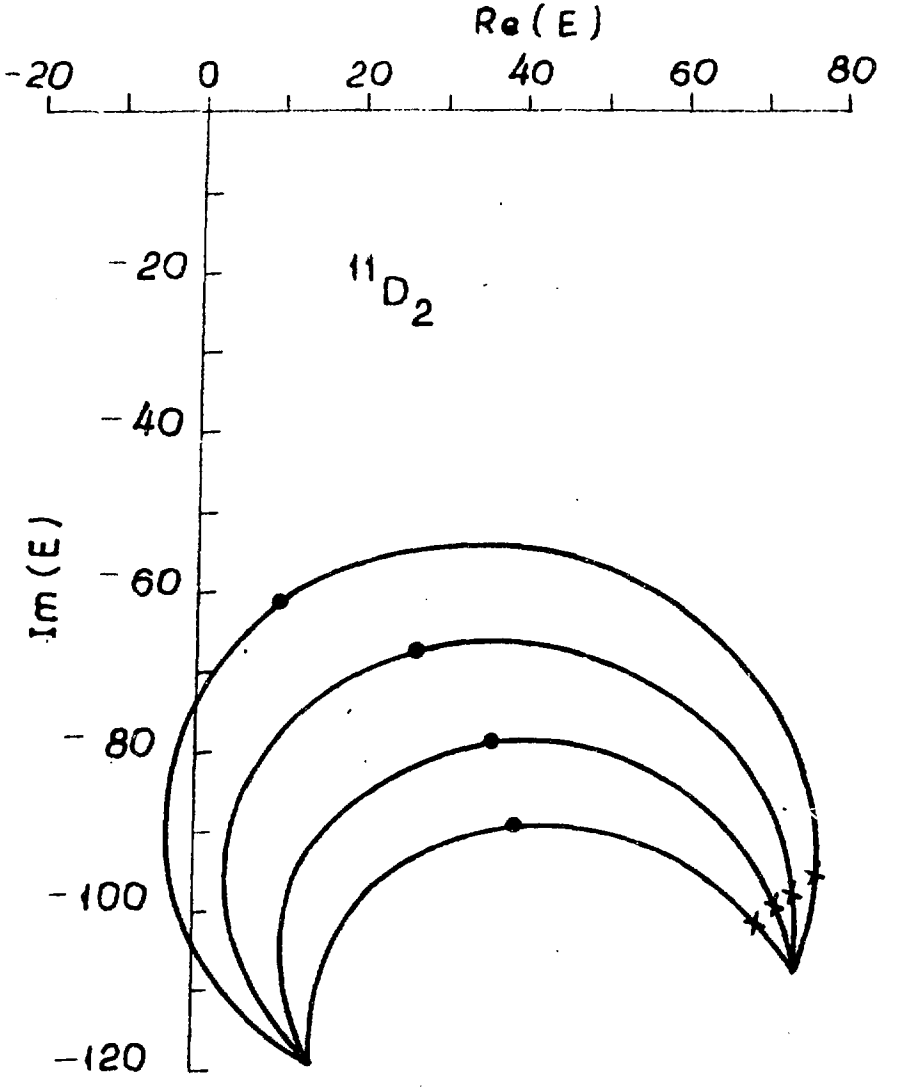

Fig. .14. As in Fig. 1 2for $^{n}D_2$ - state.

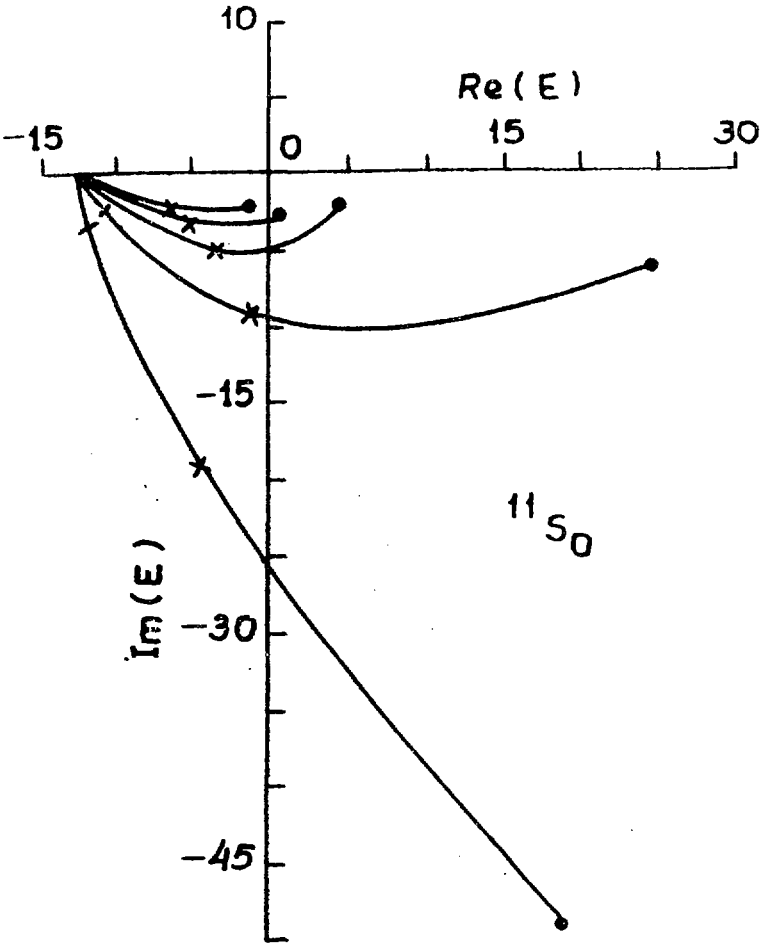

Fig. 15. The CC - pole trajectories for the $^{11}S_0$ - state in the energy plane (in MeV). Curves from top to bottom correspond to A = 8, 6, 4, 2 and 0 respectively. Positions corresponding to $\lambda \cdot 10^{-6}$ = 1, 2 and 10 are marked by • , x and — respectively.

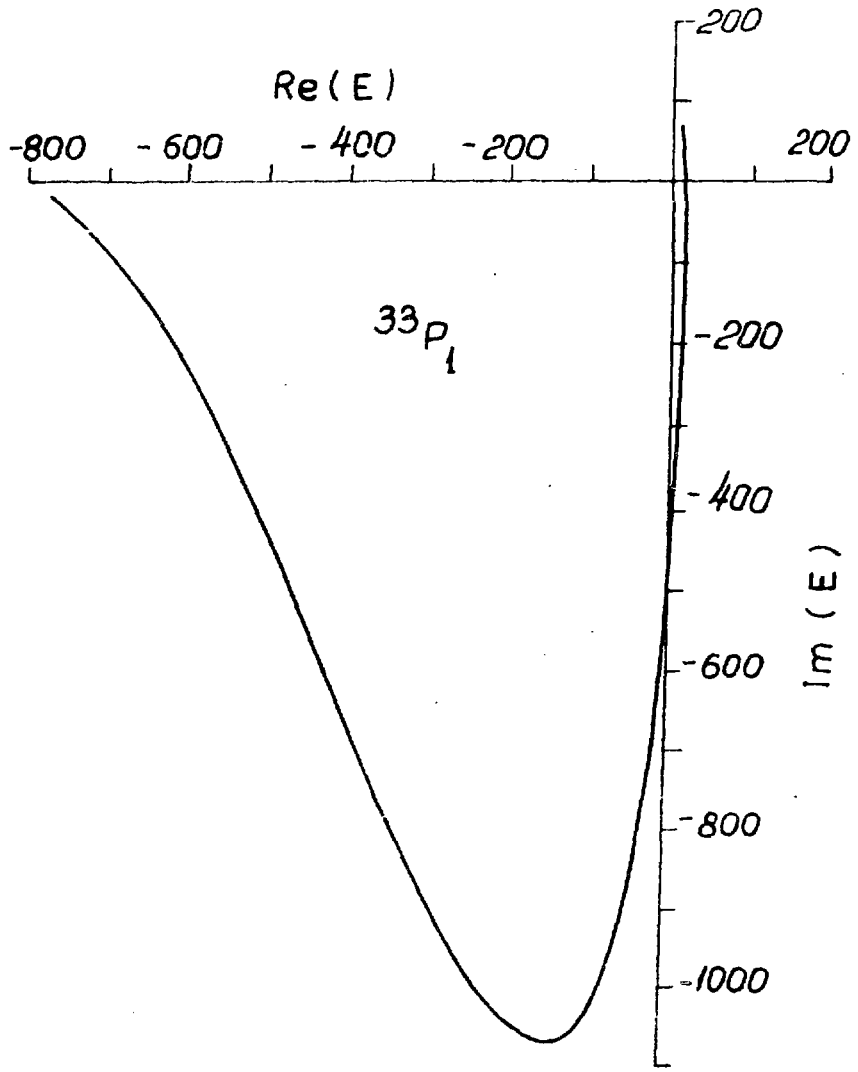

Fig. 16. A BW* - trajectory for the $^{33}P_1$ - state in the energy-plane (in MeV) for A = 3.24. The values of $\lambda \cdot 10^{-6}$ = 0.5, 1 and 10 are marked by X , • and ▲ respectively.

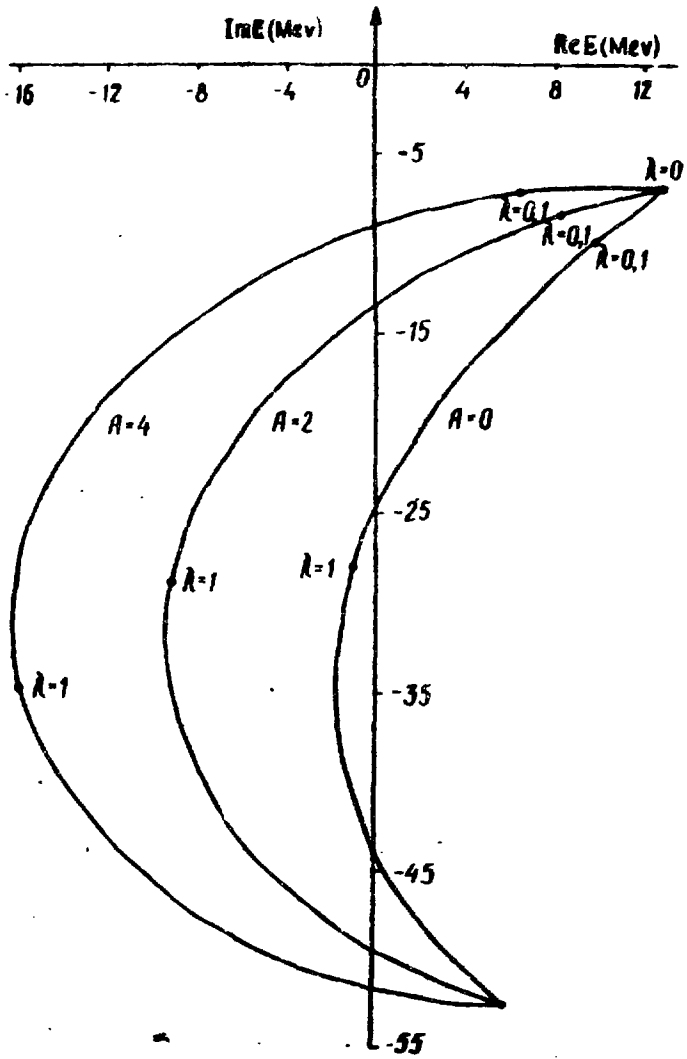

Fig. 17) BW - trajectories for the $^{11}P_1$ - state in the energy-plane (in MeV).

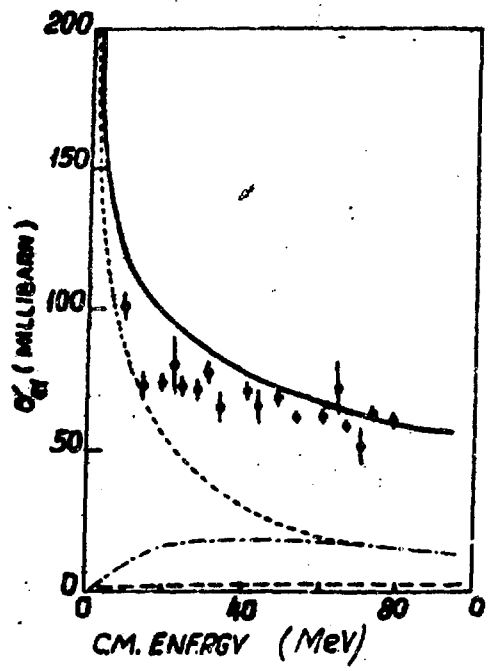

Fig. 18 The elastic $N\bar{N}$ cross section from the N/D calculations [35]. Dashed, dotted and dashed dotted curves correspond to $J = 0$, 1 and 2 contributions. Experimental points are from refs. [173] and [174].

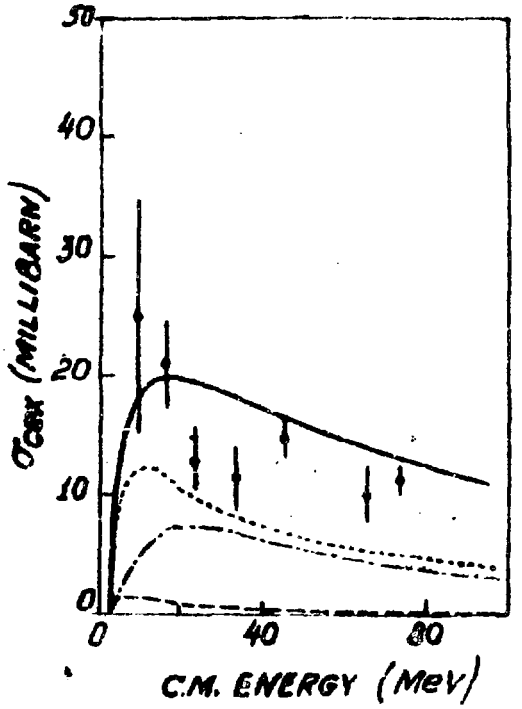

Fig. 19. As in Fig. 18 for the charge exchange cross section.

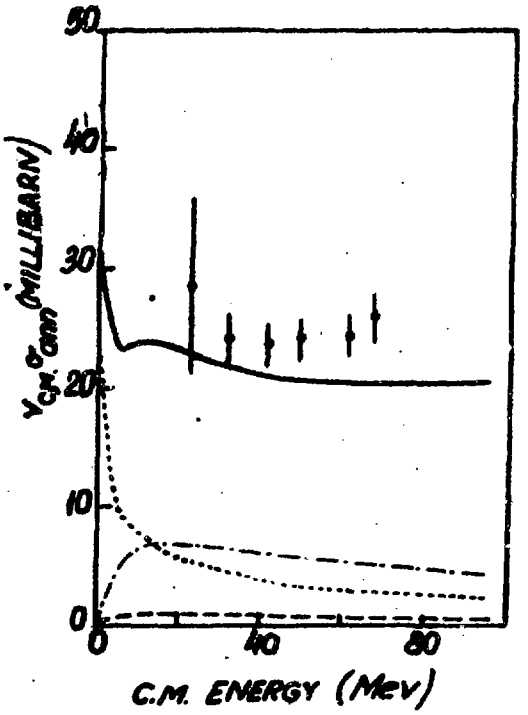

Fig. 1.20. As in Fig. 1.18 for annihilation cross section.

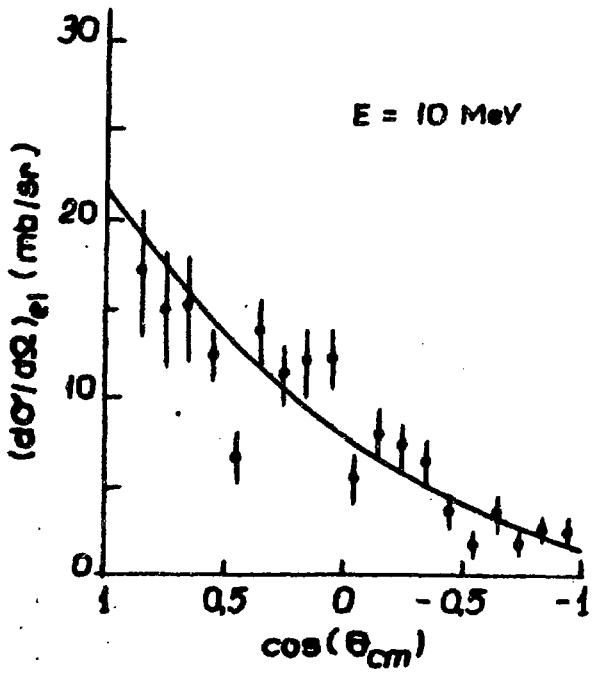

Fig. 5.21. Angular distribution of the elastic and the charge exchange scattering at E = 10 MeV. Experimental points are from ref. [175].

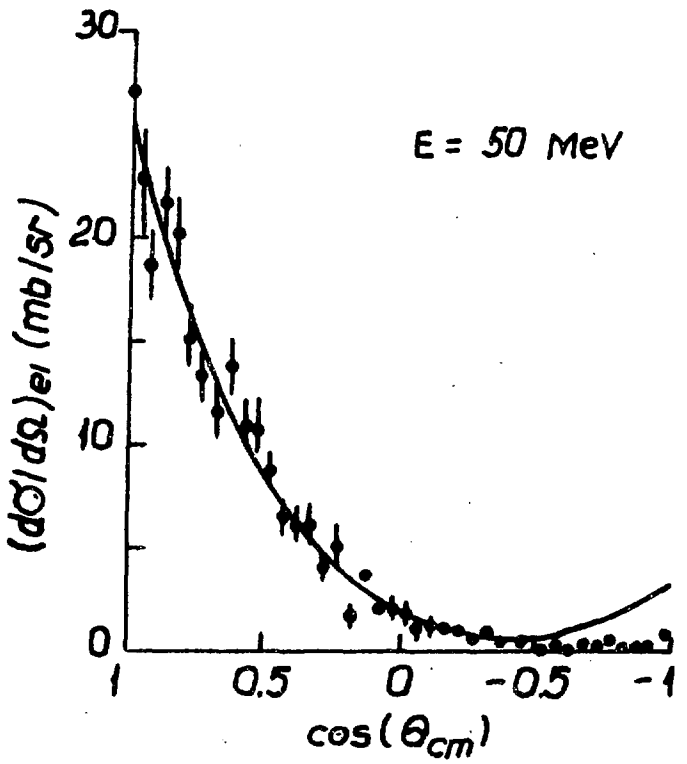

Fig. 22 As in Fig. 21 for E = 50 MeV. Experimental points are from refs. [176] and [177].

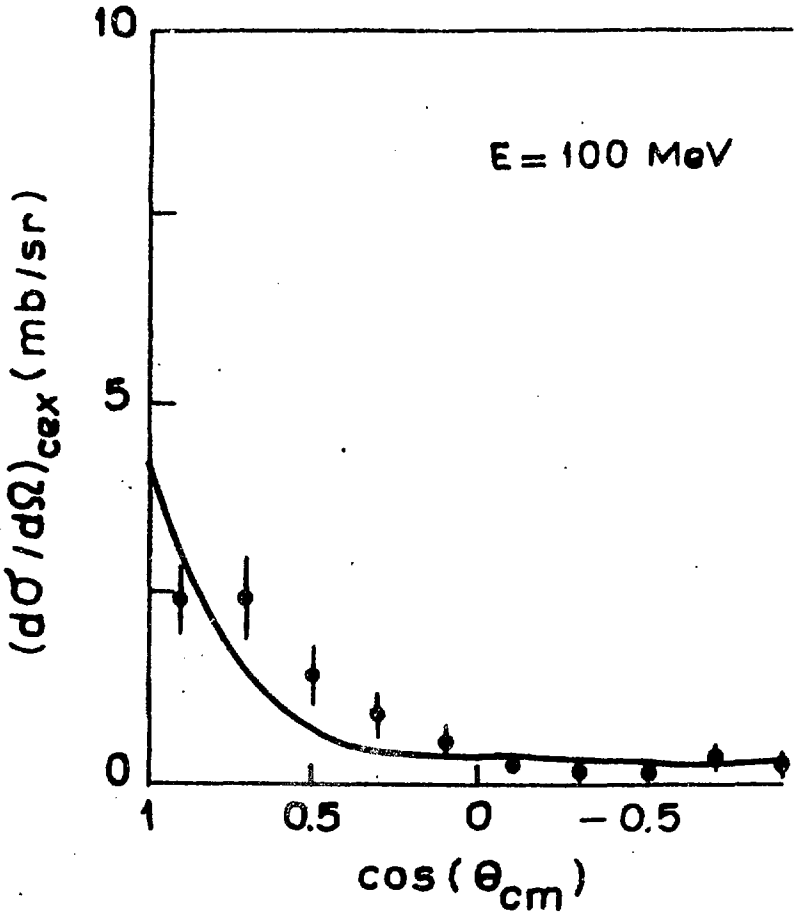

Fig. 23 Angular distribution of the charge exchange scattering at E = 100 MeV. Experimental points are from refs. [177] and [178].

References

1 J.Blatt and V.Weisskopf, Theoretical Nuclear Physics, chapt. VIII, § 7; John Wiley & Sons, Inc., New York (1952).

2 P.L.Kapur and R.E.Peierls, Proc. Roy. Soc. A166 (1938) 277.

3 E.P.Wigner and L.Eisenbud, Phys. Rev. 72 (1947) 29.

4 J.Humblet and L.R.Rosenfeld, Nucl. Phys. 26 (1961) 529.

5 H.Feshbach, Ann. Phys. (N.Y.) 5 (1958) 357.

6 H.Feshbach, Ann. Phys. (N.Y.) 19 (1962) 287; 43 (1967) 410.

7 A.M.Lane and R.G.Thomas, Rev. Mod. Phys. 30 (1958) 257.

8 H.A.Weidenmüller, Ann. Phys. (N.Y.) 28 (1964) 60.

9 T.Tamura. Phys. Rep. 14 (1974) 59.

10 E.P.Wigner, Phys. Rev. 70 (1946) 15.

11 R.H.Dalitz and S.Tuan, Ann. Phys. (N.Y.) 10 (1960) 307.

12 M.H.Ross and G.L.Shaw, Ann. Phys. (N.Y.) 13 (1961) 147.

13 R.H.Dalitz, Strange Particles and Strong Interactions, Oxford University Press (1962).

14 R.H.Dalitz, Rev. Mod. Phys. 33 (1961) 471.

15 R.G.Newton, Ann. Phys. (N.Y.) 4 (1959) 29; J. Math. Phys. 2 (1961) 188.

16 L.Fonda and R.G.Newton, Ann. Phys. (N.Y.) 10 (1960) 490 and ibid 9 (1960) 416.

17 L.Fonda and R.G.Newton, Phys. Rev. 119 (1960) 1394.

18 R.G.Newton, Scattering Theory of Waves and Particles, Mc Graw-Hill Book Co., New York, 1966.

19 W.R.Frazer and A.W.Hendry, Phys. Rev. 134B (1964) 1307.

20. L.Landau and E.Lifshitz, Theoretical Physics, P.IV, "Relativistic Quantum Theory" by V.B.Berestetsky, E.Lifshitz and L.P.Pitaevsky, part I, chapt.VII. Pergamon Press.
21 G.F.Chew, The Analytic S- Matrix, New York (1966).
22 A.D.Martin and T.D.Spearman, Elementary particle theory, North Holland Publ. Co., Amsterdam, 1970.
23 M.Kato, Ann. Phys. (N.Y.) 31 (1965) 130.
24 K.J.Le Coutour, Proc. Roy. Soc. A256 (1960) 115.
25 P.W.Johnson and R.L.Warnock, Preprint LBL-8833 (1979)
26 R.J.Eden and J.G.Taylor, Phys. Rev. Lett. 11 (1963) 516; Ph. Rev. 133 (1964) B1575
27 R.E.Peierls, Proc. Roy. Soc. 253 (1959) 16.
28 S.T.Ma, Phys. Rev. 71 (1947) 195.
29 A.I.Baz', Ya.B.Zeldovich and Perelomov, Scattering, reactions and decays in nonrelativistic quantum mechanics, Ierusalem, 1964.
30 R.H.Dalitz, invited paper at the Seminar on Kaon-Nucleus Interaction and Hypernuclei, Zvenigorod, 1977; preprint of Oxford University (1978).
31 R.J.Oakes and C.N.Jang, Phys. Rev. Lett. 11 (1963) 174.
32 D.Amati, Phys. Lett. 7 (1963) 290;
R.H.Dalitz and G.Rajasekaran, Phys. Lett. 7 (1963) 373;
M.Nauenburg and J.C.Nearing, Phys. Rev. Lett. 12 (1963) 63; M.Ross, Phys. Rev. Lett. 11 (1963) 450;
P.V.Landshoff, Nuovo Cim. 31 (1963) 697;
C.R.Hagen, Phys. Rev. Lett. 12 (1964) 1531.
33 A.M.Badalyan, M.I.Polikarpov and Yu.A.Simonov, Phys. Lett. B76 (1978) 277.
34 A.M.Badalyan, M.I.Polikarpov, Yu.A.Simonov, M.van der Velde, Proc. of the 4th European antiproton symposium, Strasbourg 1978, vol.I, p.61.

35 I.C.H.van Doremalen, Yu.A.Simonov and M.van der Velde, Phys. Lett. 87B (1979) 315.

36 I.C.H.van Doremalen, Yu.A.Simonov and M.van der Velde, Nucl. Phys. B 168 (1980) 283

37 M.I.Polikarpov and Yu.A.Simonov, preprint ITEP-162, 1978.

38 Yu.A.Simonov and J.A.Tjon, Nucl. Phys. A319 (1979) 429.

39 A.M.Badalyan, M.I.Polikarpov and Yu.A.Simonov, preprint ITEP-120 (1978).

40 W.Heitler, Proc. Cambr. Phil. Soc. 37 (1941) 291.

41 G.Brei and E.P.Wigner, Phys. Rev. 49 (1936) 519, 642; N.Bohr, Nature 137 (1936) 344.

42 L.Landau and E.M.Lifshitz, Quantum mechanics, Moscow, 1963

43 A.D.Martin, E.N.Ozmutlu and E.J.Squires, Nucl. Phys. B121 (1977) 514.

44 S.T.Ma, Austr. J. of Phys. 7 (1954) 365.

45 M.I.Polikarpov, Thesis, ITEP, Moscow, 1979.

46 M.van der Velde, Thesis, University of Amsterdam, 1980.

47 B.Hyams et al., Nucl. Phys. B64 (1973) 134.

48 G.Grayer et al., Nucl. Phys. B75 (1974) 189.

49 G.Grayer et al., Intern. Conf. on $\pi\pi$ scattering and associated topics, Tallahassee (1973); AIP Conf. Proc. (N.Y.) 13 (1973) 117.

50 P.Estabrooks et al., AIP Conf. Proc (N.Y.) 13 (1973) 37.

51 D.M.Biennie et al., Phys. Rev. Lett. 31 (1973) 1534; Phys. Rev. D8 (1973) 2789.

52 M.Aguilar-Benitez et al., preprint CERN/EP/Phys - 78-5.

53 M.Cerrada et al., Phys. Lett. B62 (1976) 353.

54 A.D.Martin, Nuovo Cim., 7 (1958) 607

55 A.D.Martin and E.N.Ozmutlu, Nucl. Phys. B158 (1979) 520.

56 S.D.Protopopescu et al., Phys. Rev. D7 (1973) 1279.

57 Y.Fujii and M.Fukugita, Nucl. Phys. B85 (1975) 179.

58 J.L.Peterson, preprint CERN-77-04.

59 D.Morgan, Phys. Lett. B51 (1974) 71.

60 S.M.Flatté, Phys. Lett. B63 (1976) 224, 228.

61 P.Plano, Proc. XV Intern. Conf. on High Energy Physics, Naukova Dumka (1972) 148.

62 C.E.Jones, Ann. Phys. (N.Y.) 31 (1965) 481.

63 L.Gauthier and A.N.Kamal, Ann. Phys. (N.Y.) 88 (1974) 193; 90 (1975) 515.

64 L.Fonda, Scattering Theory, ed Barut, A.O.Gordon and Breach (1969) 130-139 and references therein.

65 P.R.Graves-Morris, Ann. Phys. (N.Y.) 41 (1967) 477.

66 C.Hategan, Ann. Phys. (N.Y.) 116 (1978) 77.

67 M.S.Ata and C.Hategan, Rev. Roum. Phys. 24 (1979) 3.

68 Z.E.Switowski, J.C.P.Heggie and F.M.Mann, Phys. Rev. C17 (1978) 392.

69 Z.E.Switowski et al., Aust J.Phys. 31 (1978) 253.

70 V.S.Barashenkov, V.D.Toneev "Interaction of high energy particles ...", Moscow (1972)

71 J.L.Zyskind, Nucl. Phys. A301 (1978) 179.

72 M.Eyb and H.Hofmann, J.Phys. B8 (1975) 1095.

73 L.D.Blokhintzev and Yu.A.Simonov, preprint ITEP-33(1978).

74 L.D.Blokhintzev and Yu.A.Simonov, Theor. Math. Phys. (USSR) 36 (1978) 64.

75 R.Engelmann et al., Phys. Lett. B21 (1966) 587.

76 F.Eisele et al., Phys. Lett. B37 (1971) 204.

77 G.Alexander et al., Phys. Rev. 173 (1968) 1452.

78 B.Sechi-Zorn et al., Phys. Rev. 175 (1968) 1735.

79 R.H.Dalitz, R.C.Herdon, Y.C.Tang, Nucl. Phys. B47 (1972) 109.

80 O.I.Dahl et al., Phys. Rev. Lett. 6 (1961) 142;
D.Cline, R.Laumann and J.Mapp, Phys. Rev. Lett. 20 (1968) 1452.
81 Tai Ho Tan, Phys. Rev. Lett. 23 (1969) 395.
82 D.Eastwood et al., Phys. Rev. D3 (1971) 2603.
83 O.Braun et al., Nucl. Phys. B124 (1977) 45.
84 D.P.Goual and A.V.Sodhi, Phys. Rev. D18 (1978) 948.
85 R.A.Burnstein et al., Phys. Rev. 177 (1969) 1945.
86 J.A.Kadyk et al., Nucl. Phys. B 27 (1971) 13.
87 M.M.Nagels, T.A.Rijken and J.J.de Swart, Phys. Rev. D20 (1979) 1633.
88 M.M.Nagels et al., preprint University of Nijmegen, THEF-78-4;
M.M.Nagels, Thesis, University of Nijmegen, 1975.
89 M.M.Nagels et al., Nucl. Phys. B147 (1979) 189.
90 Tai Ho Tan, Phys. Rev. D7 (1973) 600.
91 H.G.Dosch and V.Hepp, Phys. Rev. D18 (1978) 4071;
H.G.Dosch and I.O.Stamatescu, preprint HD-THEP-9 (1979).
92 A.Nishimura, preprint UT-309 (1978).
93 V.Bargmann, Proc. Acad. Sci. USA 38 (1952) 961.
94 F.Calogero, Nuovo Cim. 36 (1965) 199.
95 A.Bohr and B.R.Mottelson, Nuclear Structure, VI, Benjamin Inc. 1969.
96 I.S.Shapiro, Phys. Rep. 035 (1978) 129.
97 A.N.Kamal and M.J.Kreutzer, Phys.Rev. D2 (1970) 2033.
98 F.Myhrer and A.W.Thomas, Phys.Lett. B64 (1976) 59.
99 B.R.Karlsson and B.O.Kerbikov, Nucl. Phys. B141 (1978) 241.
100 L.P.Kok and H.van Haeringen, preprint of Groningen University (1980).

101 F.Myhrer and A.Gersten, Nuovo Cim. 37A (1977) 21.

102 R.A.Bryan and R.J.N.Phillips, Nucl. Phys. B5 (1968)201.

103 T.Ueda, preprint OVAM-79-5-5, 1979.

104 S.Joffily, Nucl. Phys. A215 (1973) 301.

105 R.G.Gordon, J.Chem.Phys. 52 (1970) 6211;
M.Baer and D.J.Kouri, J.Chem.Phys. 57 (1972) 3441;
D.J.Ernst et al., Phys. Rev. C10 (1974) 1708;
R.B.Gerber and N.C.Rosenbach, Phys. Rev. A9 (1974) 301.

106 B.McKellar, J.Phys.G: Nucl.Phys. 1 (1975) 180.

107 L.H.Schick, Phys. Rev. C12 (1975) 523;
L.H.Schick and N.K.Tyagi, Phys. Rev. D5 (1972) 1794;
E.Satoh and Y.Nogami, Phys. Lett. B32 (1970) 243.

108 L.H.Schick and A.S.Toepfer, Phys. Rev. 170 (1968) 946.

109 P.Beregi and I.Lovas, Phys. Lett. B33 (1970) 150.

110 K.King and B.H.J.McKellar, Phys.Rev. C9 (1974) 1309.

111 A.D.McKellar and M.Coz, Nucl. Phys. A269 (1976) 1.

112 K.F.Ratcliff and N.Austern, Ann.Phys. (N.Y.) 42
(1967) 185.

113 R.H.Lemmer and G.C.Shakin, Ann.Phys. (N.Y.) 27
(1964) 13.

114 I.Lovas, Madyar Fiz. Foly. 13 (1965) 319.

115 O.Mikoshiba, T.Terasawa and M.Tanifuji, Nucl. Phys.
A168 (1971) 417;
J.T.Reynolds et al., Phys. Rev. 176 (1968) 1213.

116 J.T.Brown, B.W.Downs and C.K.Iadings, Ann. Phys.
(N.Y.) 60 (1970) 148.

117 F.Gutbrod, G.Kramer and Ch.Rumpf, preprint DESY
78-48 (1978);

118 A.M.Lane and P.Robson, Phys. Rev. 151 (1966) 774.

119 J.L.Roeder, Ann. Phys. (N.Y.) 43 (1967) 382.

120 M.Bolterli and A.S.Rinat, Phys. Rep. C15 (1977) 42.

121 G.Risent and S.S.Armad, Nuovo Cim. 12A (1972) 665.

122 G.Cattapan, G.Risent and V.Vanzani, Nuovo Cim. 33A (1976) 703.

123 J.Quantanilla and P.A.Mello, Ann. Phys. 75 (1973) 332.

124 Yu.A.Simonov, Yad Fiz. 3 (1966) 630;
A.M.Badalyan and Yu.A.Simonov, Yad. Fiz. 3 (1966) 1032.
Yu.A.Simonov, The Hyperspherical Expansion Approach to Nuclear Bound States, pp.527-564 from Nuclear Many-Body Problem, by F.Calogero and C.Ciofi Degli Atti, Rome (1972) 3.

125 B.O.Kerbikov, preprint ITEP-37, 1979.

126 A.E.Kudryavtsev and R.T.Tyapaev, Yad. Fiz. 30(1979)1609.

127 L.N.Bogdanova, V.E.Markushin and I.S.Shapiro, preprint ITEP-7 (1979).

128 L.N.Bogdanova and V.E.Markushin, preprint ITEP-120,1979.

129 G.Chew and S.Mandelstam, Phys. Rev. 119 (1960) 467.

130 J.D.Bjorken, Phys. Rev. Lett. 4 (1960) 473;
J.D.Bjorken and M.Nauenberg, Phys. Rev. 121 (1961)1250.

131 A.Martin, Phys. Rev. 124 (1961) 614.

132 C.B.Dover and J.M.Richard, Ann. Phys. (N.Y.)121(1970)70.

133 W.W.Buck, C.B.Dover and J.M.Richard, Ann. Phys. (N.Y.) 121 (1979) 47.

134 M.I.Polikarpov and M.van der Velde, preprint of University der Vrije (1979)

135 G.Breit, E.Condon and R.Present, Phys. Rev. 50 (1936) 825;
G.Breit, B.Thaxton and L.Eisenbud, Phys. Rev. 55 (1939) 1018.

136 L.Landau and Yu.Smorodinsky, JETP 14 (1944) 269.

137 H.A.Bethe, Phys. Rev. 76 (1949) 38;
G.F.Chew and M.L.Goldberger, Phys. Rev. 76 (1949) 1637;
F.Barker and R.E.Peierls, Phys. Rev. 75 (1949) 3122.

138 E.Lambert, Helv. Phys. Acta, 42 (1969) 667.

139 A.M.Badalyan and Yu.A.Simonov, Yad. Fiz. 11 (1970) 1318.

140 A.E.Kudryavtsev and V.S.Popov, JETP Lett. 29 (1979) 311;
V.S.Popov. A.E.Kudryavtsev and V.D.Mur, JETP 77
(1979) 1727.

141 V.D.Mur et al., JETP Lett. 31 (1980) 429 and preprint
ITEP-46, 1980.

142 S.Deser et al., Phys. Rev. 96 (1954) 774.

143 Ya.Zeldovich, Sov. Phys. Solid. State 1 (1959) 1637.

144 M.Krell, Phys. Rev. Lett. 26 (1971) 584.

145 K.A.Brueckner, R.Serber and K.M.Watson, Phys. Rev.
81 (1951) 575;
K.A.Brueckner, Phys. Rev. 84 (1952) 258.

146 A.D.Martin, Phys. Lett. B65 (1976) 346.

147 M.Abramowitz and I.A.Stegun, editors, Handbook of
Mathematical functions (Dover, New York, 1965).

148 V.S.Popov, JETP 60 (1971) 1228.

149 A.E.Kudryavtsev et al., Sov.Phys. JETP 47 (1978) 225.

150 J.H.Koch, M.M.Sternheim and J.F.Walker, Phys.Rev.Lett.
26 (1971) 1465, Phys. Rev. C5 (1972) 381.

151 J.D.Jackson, in Proc. Sum. Inst. on Part Phys.,
August 1970, SLAC-198.

152 A.M.Badalyan and Yu.A.Simonov, Sov.J.Part.Nucl.
6 (1975) 119;
S.I.Manaenkov, Theor.Math.Phys. 12 (1972) 397.

153 B.O.Kerbikov, JETP Lett. 30 (1979) 22; preprint
ITEP-125, 1979.

154 F.Peregi, Nucl. Phys. A206 (1973) 217.

155 L.P.Kok, J.W.de Maag and Yu.A.Simonov, preprint Groningen Univ., 1980.

156 H.Haeringen, Nucl. Phys. A253 (1975) 355.

157 H.Haeringen and L.P.Kok, preprint Groningen Univ.1980.

158 E.Fermi and C.N.Yang, Phys. Rev. 89 (1949) 1256.

159 A.M.Afrikyan, Sov. Phys. JETP 3 (1956) 503.

160 H.Bethe and R.Hamilton, Nuovo Cim. 4 (1956) 1.

161 J.S.Ball and G.F.Chew, Phys. Rev. 109 (1958) 1385.

162 J.S.Ball, A.Scotti and D.Y.Wong, Phys. Rev. 142 (1966) 1000.

163 L.N.Bogdanova, O.D.Dalkarov and I.S.Shapiro, Ann.Phys. 84 (1974) 261.

164 L.N.Bogdanova, O.D.Dalkarov and I.S.Shapiro, ZhETF 70 (1976) 805.

165 G.C.Rossi and G.Veneziano, to be published in Phys.Rep.

166 M.L.Goldberger and K.M.Watson, Collision theory, J.Wiley ans Sons, inc. 1964, New-York - Toronto.

167 B.O.Kerbikov et al., preprint ITEP-61, 1978.

168 B.O.Kerbikov and I.S.Shapiro, preprint ITEP-159, 1978.

169 L.Montanet, to be published in Phys.Rep.

170 R.Vihn Mau, Proc. of the workshop on baryonium ... , ed. by B.Nicolescu et al.

171 A.M.Green, M.E.Sainio and S.Wycech, preprint Univ. of Helsinki (1979)
A.M.Green, M.E.Sainio and J.M.Richard, preprint Univ. of Helsinki, 1979 and private communications.

172 R.Muirhead, Proc. of the 4th Europ. antiproton Symp., Strassbourg, 1978.

173 J.E.Enstrom, et al., $\bar{N}$ - N and $\bar{N}$ - d interactions - a compilation, LBL-58, May 1972.

174 M.Alston-Garnjost et al., Phys.Rev.Lett. 35 (1975) 1685.

175 D.Spencer and D.N.Edwards, Nucl. Phys. B19 (1970) 501.

176 B.Conforto et al., Nuovo Cim. 54 A (1968) 441.

177 R.Bizzari et al., Nuovo Cim. 54A (1968) 456.

178 D.Cline et al., Phys. Rev. Lett. 21 (1968) 1268.

ИНДЕКС 3624